DNA methylation-associated dysregulation of *ANGPTL4* and *TUBB2A* in acute myeloid leukemia

Mat Jusoh Siti Asmaa[1], Faezahtul Arbaeyah Hussain[2,5], Azlan Husin[3,5], Shaharum Shamsuddin[4], Muhammad Farid Johan[1]

[1]Department of Haematology, School of Medical Sciences, Universiti Sains Malaysia, 16150 Kubang Kerian, Malaysia

[2]Department of Pathology, School of Medical Sciences, Universiti Sains Malaysia, 16150 Kubang Kerian, Malaysia

[3]Department of Internal Medicine, School of Medical Sciences, Universiti Sains Malaysia, 16150 Kubang Kerian, Malaysia

[4]School of Health Sciences, Universiti Sains Malaysia, 16150 Kubang Kerian, Malaysia

[5]Hospital Pakar Universiti Sains Malaysia, 16150 Kubang Kerian, Malaysia

*Corresponding author:
Muhammad Farid Johan
faridjohan@usm.my

Received 28 Nov 2024.
Revised 10 July 2025.
Accepted 11 Aug 2025.
Published Online 01 Oct 2025

Abstract - Acute myeloid leukemia (AML) is a clonal hematological malignancy marked by genetic and epigenetic alterations. Epigenetic modifications, such as DNA hypermethylation and histone changes, may drive the silencing of tumor suppressor genes (TSGs), a key feature of AML pathogenesis. Angiopoietin-like 4 (ANGPTL4) and tubulin Beta 2A (TUBB2A) genes were identified through transcriptomic analysis of Kasumi-1, an AML cell line, following treatments with epigenetic modulators: Trichostatin A (TSA) and 5-Azacytidine (5-Aza). ANGPTL4, involved in lipid metabolism, promotes tumor growth, metastasis, and angiogenesis, while TUBB2A, part of the microtubule network, is linked to cancer when dysregulated. This study investigates the expression and methylation status of ANGPTL4 and TUBB2A in AML patients, and examines the expression of ANGPTL4, TUBB2A, and histone H3 and H4 proteins in the Kasumi-1 cells treated with a specific agent. Quantitative real-time PCR (qPCR) was performed in 52 de novo AML patients with varying cytogenetic abnormalities. Bisulfite sequencing PCR (BSP) was performed in a representative subset of patients (n = 12). Protein expression of ANGPTL4, TUBB2A, and histone H3 and H4 was analysed by Western blot. The results showed reduced expression of ANGPTL4 in 98.0% of AML patients (median <0.001) and TUBB2A in 73.1% (range 0.33–0.77), with most cases of downregulated TUBB2A found in cytogenetically normal (CN) patients. Bisulfite sequencing revealed fully methylated CpG regions in 96.1% of ANGPTL4 and 54.9% of TUBB2A. Western blot analysis showed the upregulation of ANGPTL4 and TUBB2A proteins, underscoring their functional relevance. Additionally, increased levels of core histones H3 and H4 following TSA treatment suggested an upregulation of global histone gene expression in response to HDAC inhibition. These findings indicate that the underexpression of ANGPTL4 and TUBB2A in AML patients may be a consequence of aberrant hypermethylation of their promoter regions. The downregulation of these genes could support the persistence of leukemic stem cells. Further study on the epigenetic mechanisms underlying the downregulation of ANGPTL4 and TUBB2A in AML is recommended.

***Keywords* — Acute myeloid leukemia, Angiopoietin-like 4, Bisulfite sequencing, DNA Methylation, *TUBB2A*.**

1 INTRODUCTION

Acute myeloid leukemia (AML) is a clonal hematopoietic disorder caused by genetic alterations of crucial genes involved in cell proliferation, differentiation, apoptosis, and gene transcription, which disrupt normal hematopoiesis [1]. The developmental arrest in hematopoietic cells is considered a hallmark in AML pathogenesis, and subsequent mutations provide a proliferative advantage to these clonal cells, contributing to leukemogenesis. Over the years, the role of epigenetics in cancer development has garnered significant attention, highlighting the stable and heritable modifications of gene function that occur during cell division [2]. Epigenetic changes, including nucleosome positioning, non-coding RNAs, DNA methylation, and histone modifications are fundamental to cancer development and progression [3]. These changes can activate oncogenes and silence tumor suppressor genes (TSGs), resulting in increased plasticity of cellular structure and function that drives cancer development [4]. Among these, shifts in DNA methylation and histone modification patterns are the most common epigenetic mechanisms and a promising target for drug development [5].

In AML and other cancer cells, DNA methylation is the most studied epigenetic inactivation mechanism linked to gene silencing, leading to transcriptional deactivation [6]. It is a process by which a methyl group (CH_3) is bound to the 5' position of the cytosine ring within CpG dinucleotides, catalyzed by DNA methyltransferases (DNMTs). Transcriptional silencing of a particular gene served as a consequence of the abnormal methylation pattern [7]. DNA methylation conserves genome integrity

and regulates genomic imprinting to control gene transcription and cellular development [8]. Silencing of TSGs by hypermethylation is a universal common cause of events in practically all types of cancer, including leukemia [9]. It is believed to be an early event in leukemogenesis that involves genes associated with growth factors, cytokines, and signal transduction molecules, as well as those regulating cell cycle and apoptosis.

Histone modifications, primarily through acetylation, play crucial roles in regulating chromatin structure and gene expression. Two enzymes regulated histone acetylation activity: histone acetylases (HATs) and histone deacetylases (HDACs). Acetylation of histones H3 and H4 is generally associated with transcriptional activation [10]. Abnormalities in the acetylation activity of histones alter cellular and metabolic processes by either repressing or upregulating gene transcription [11]. The fusion protein of promyelocytic leukemia–retinoic acid receptor-α (PML-RARα) in acute promyelocytic leukemia (APL) can abnormally reactivate histone deacetylases HDACs, consequently inhibiting gene transcription and leading to failure in cellular differentiation [12].

Previously, we identified two potential TSGs: angiopoietin-like 4 (*ANGPTL4*) and tubulin beta 2A class IIa (*TUBB2A*) through gene expression profiling analysis of Kasumi-1 cells [an AML cell line with t(8;21)/AML1-ETO] treated with epigenetic-modulating agents: Trichostatin A (TSA), 5-azacytidine (5-Aza), and/or in combination of TSA/5-Aza, which may have epigenetic implications in AML signalling. TSA acts as an HDAC inhibitor, which inhibits HDAC activity. 5-Aza serves as a DNA methylation inhibitor, functioning as a DNA demethylating agent. Our study showed that *ANGPTL4* and *TUBB2A* were significantly re-expressed genes with high fold change differences after treatment with TSA (fold change, *ANGPTL4*: 791.26 and *TUBB2A*: 574.87, $p < 0.05$), and combination treatment with TSA and 5-Aza (fold change, *ANGPTL4*: 429.s well as in and *TUBB2A*: 435.79, $p < 0.05$). During 5-Aza treatment, these genes were commonly re-expressed (fold changes in *ANGPTL4*: 2.67 and *TUBB2A*: 2.67, $p < 0.05$), as validated by quantitative real-time PCR (qRT-PCR) [13]. Based on these findings, it was suggested that *ANGPTL4* and *TUBB2A* could be putative TSGs that may play a role in epigenetic mechanisms, contributing to the control of gene expression in AML.

ANGPTL4 (Entrez gene ID: 51129) encodes a glycosylated, secreted protein with a fibrinogen-like C-terminal domain, primarily induced by the nuclear receptor protein peroxisome-proliferator-activated receptor (PPAR). The gene is located on chromosome 19p13.2 and plays key roles in regulating lipid metabolism, glucose homeostasis, and insulin sensitivity. The 45,214 Dalton protein may function as a survival factor for vascular endothelial cells and inhibit metastasis by suppressing vascular growth and tumor cell invasion [14]. *ANGPTL4* is among the 1217 human TSGs that are consistently regulated in 11 cancer types, as reported by the Tumor Suppressor Gene (TSGene) version 2.0 database, provided by the University of Texas (https://bioinfo.uth.edu/TSGene/) [15, 16].

TUBB2A (Entrez gene ID: 7280) encodes a class II β-tubulin, one of six tubulin families—alpha (α), beta (β), gamma (γ), delta (δ), epsilon (ε), and zeta (ζ) that serve as key components of microtubules. This gene is located on chromosome 6p25.2 and is involved in regulating cytoskeletal organization, microtubule-based processes, and the mitotic cell cycle. It encodes a 49,907 Dalton protein that plays a role in small GTPase activity, GTP binding, nucleotide binding, as well as acetylation and methylation [17]. In addition, a previous study has demonstrated that both *ANGPTL4* and *TUBB2A* were among the predicted and reliable putative TSGs involved in the pathogenesis of cancer, as screened via a computational method, random walk with restart (RWR) network diffusion algorithm executed on a protein-protein interaction (PPI) network [18].

The present study investigates the expression levels and methylation status of *ANGPTL4* and *TUBB2A* in AML patients. A total of fifty-two AML patients with diverse cytogenetics were analysed using qRT-PCR to assess gene expression. At the same time, bisulfite sequencing was employed to evaluate the methylation status of *ANGPTL4* and *TUBB2A* in a representative sample of AML patients. These findings suggest that hypermethylation of *ANGPTL4* and *TUBB2A* gene promoters may be associated with reduced gene expression in AML, with potential involvement of histone modifications in regulating their transcription. This report will primarily present findings on the novel

function of both *ANGPTL4* and *TUBB2A,* specifically their roles in the epigenetic control of gene expression in AML.

2 MATERIALS AND METHODS

2.1 BLOOD SAMPLE COLLECTION

Fifty-two blood samples, comprising either peripheral blood (PB) or bone marrow aspirates, were collected with informed consent from newly diagnosed AML patients between 2010 and 2017 at the Molecular Unit of the Haematology Laboratory, Hospital Universiti Sains Malaysia (USM), Malaysia. The patient's demographics and clinical data were retrieved from the Haematology Patient Information System (HPIS) v4.2, USM. The patient's cytogenetic profiles were obtained from the Human Genome Centre, USM. PB was collected from twenty screened healthy blood donors at the Blood Transfusion Unit of Hospital USM, following informed consent, and used as a standard control. FMS-like tyrosine kinase 3-internal tandem duplication (*FLT3-ITD*) and nucleophosmin 1 (*NPM1*) mutations were previously analysed and detected in 9 (17.3%) and 8 (15.4%) cases, respectively. The USM Research Ethics Committee approved this study protocol [Ref no 224.4. (2.5)] and USM/JEPeM/16030102.

2.2 TOTAL DNA AND RNA EXTRACTION

1-3 mL of whole blood from AML patients and healthy normal controls were extracted and purified using the Wizard Genomic DNA Purification Kit and the Total RNA Isolation Kit (Promega Corp, SA, USA) according to the manufacturer's protocol. The concentration and quality of DNA and RNA were determined using a Nanodrop ND-1000 spectrophotometer (Thermo-Fisher Scientific, Inc., WA, USA). Ratios between 1.7 and 1.9 at A260/280 were considered indicative of high-purity samples. Their integrity was analysed by 1.5% agarose gel electrophoresis. The DNA and RNA samples were stored at -20 °C for further analysis and at -70 °C for long-term preservation.

2.3 QUANTITATIVE REAL-TIME PCR (qRT-PCR)

qRT-PCR was performed using Taqman gene expression assays, and the results were analysed by the Applied Biosystems 7500 Real-Time PCR System (Applied Biosystems, CA, USA) to measure the *ANGPTL4* and *TUBB2A* transcript levels in 52 AML patients. RNA was reverse transcribed using a High-Capacity cDNA Reverse Transcription Kit (Applied Biosystem, CA, USA). qRT-PCR assays for *ANGPTL4* and *TUBB2A* were designed by Integrated DNA Technologies (IDT) using PrimeTime® Pre-designed Assays (IDT, IA, USA) and amplified by PrimeTime® Gene Expression Master Mix (IDT, IA, USA). The reaction conditions were as follows: 95 °C for 3 minutes, followed by 40 cycles of 95°C for 15 seconds and 60 °C (annealing/extension) for 1 minute. The experiment was conducted using a relative quantitation (RQ) of duplicated samples calculated by the $2^{\Delta\Delta 2\text{-CT}}$ method ($\Delta\Delta CT$ $\Delta CT_{Patient}$-$\Delta CT_{Healthy\ control}$, $\Delta CT=Ct_{Selected\ genes}$-$Ct_{GAPDH/B2M}$, normalized to healthy controls. *B2M* and *GAPDH* were used as endogenous control genes (**Table I**).

Table I: Quantitative Real-Time PCR Primers

Pre-designed assay*			
Gene	**Assay ID**	**Nucleotide bases refererence**	**NCBI**
ANGPTL4	Hs.PT58.25480012	1843-1902	NM_139314
TUBB2A	Hs.PT58.40767003	1753-1812	NM_001069

Custom-designed primer and probe			
Gene	**Primer and probe sequences**	**Nucleotide bases**	**NCBI reference**
B2M	**Primer:**		NM_004048
	Forward: CCAGCGTACTCCAAAGATTCA	118-138	
	Reverse: TGGATGAAACCCAGACACATAG	211-190	
	Probe: ACTCACGTCATCCAGCAGAGAATGG	144 - 168	
GAPDH	**Primer:**		NM_002046
	Forward: GGTGTGAACCATGAGAAGTATGA	574-596	
	Reverse: GAGTCCTTCCACGATACCAAAG	696-675	
	Probe: AGATCATCAGCAATGCCTCCTGCA	608-631	

* Pre-designed by Integrated DNA Technologies (IDT) using PrimeTime® Pre-designed Assays (IDT, IA, USA)

2.4 BISULFITE MODIFICATION

High-purity and intact DNA with a concentration of more than 100 ng/µL from AML patients was subsequently subjected to bisulfite modification using the EZ DNA methylation-gold Kit (Zymo Research, CA, USA) according to the

manufacturer's protocol. In the procedures, sodium bisulfite was artificially added to the C-6 position of cytosine residues to mediate the conversion of unmethylated cytosines to uracil, while methylated cytosines remained unchanged. The underlying principle of this reversible chemical process is the rapid deamination of cytosines to 5, 6-dihydrouracil-6-sulfonate. The subsequent treatment with an alkaline solution swiftly eliminates the sulfonate group and regenerates the double bond, yielding uracil. When cytosines are methylated, this reaction is "blocked" due to the extremely low reaction rates for the formation of 5-methyl-6-dihydrocytosine-6-sulfonate, and they are therefore not converted to uracil.

2.5 BISULFITE SEQUENCING PCR

Bisulfite sequencing PCR (BSP) was used to analyse the DNA methylation profiles of the promoter regions of *ANGPTL4* and *TUBB2A* in a representative sample of 12 AML patients. The BSP primers were designed using MethPrimer software (http://www.urogene.org/methprimer) as summarized in **Table II**.

Table II: Bisulfite sequencing PCR primers

Gene	Sequence (5'-3')	Length & size	CpG count	NCBI Reference sequence
ANGPTL4	Forward: GGTTAGGAATTTGAGATTAGTAGAG Reverse: AAACAAAATTTCACCATATTAACCAA	1-3500 (2007-2364) 358bp	15	NG_012169.1
TUBB2A	Forward: AGATGAGTTATTTTAGGTAGGG Reverse: AAAAATAAATCCATAACAATATTCA	1-5000 (2156-2397) 242bp	12	NG_042223.1

Commercialized human methylated and non-methylated DNA (Zymo Research, CA, USA), subjected to bisulfite modification, were used as positive and negative controls, respectively. Amplification of BSP was performed in a 25 µL final volume per sample comprising 5 µL of 50 ng bisulfite-converted DNA, 12.5 µL of 1X KOD–Multi & Epi® PCR buffer (Toyobo Co., Ltd, Osaka, Japan), 1.0 µL of 0.5 µM forward and reverse primers, 0.5 µL of KOD–Multi & Epi (neutralize DNA polymerase and inhibit its 3'-5' exonuclease activities), and nuclease-free water in an ABI Veriti™ Thermal Cycler (Applied Biosystem, Foster City, USA). The reaction conditions consisted of an initial denaturation step at 94°C for 2 minutes, followed by 40 cycles of denaturation at 98°C for 10 seconds, annealing at 60°C for 30 seconds, and extension at 68°C for 30 seconds, with no final extension. Amplicons were electrophoresed on 2.5% agarose gels and visualized by ethidium bromide staining under ultraviolet transillumination for confirmation. The methylation of CpG sites was confirmed by automated DNA sequencing (1st BASE Asia). Resulted sequences were compared with the wild-type sequence, viewed, and analysed in Finch TV software Version 1.4.0 (Geospiza, Inc., USA) to determine the signal intensities of T (thymine) and C (cytosine) dinucleotide peaks throughout the CpG sites of the selected gene region. The methylation level of each CpG, as indicated by a peak difference in either cytosine or thymine dinucleotide as read from the chromatogram, was presented as a methylation percentage, as described by Parrish *et al.* [19]. In this study, the degree of methylation level was summarized in a table presented with a colour shading.

2.6 KASUMI-1 PROTEIN EXTRACTION AND MEASUREMENT OF PROTEIN CONCENTRATION

Kasumi-1 cell line was grown until it reached 70-90% confluency and at least at passage 5 (P5) after thawing. The half-maximal inhibitory concentrations (IC_{50}) of TSA and 5-Aza were 6.25 µM and 6.95 µM, respectively, as determined in a prior study. Kasumi-1 cells were treated with TSA and 5-Aza at IC_{50} concentrations in a six-well plate for 24 hours, in triplicate. Then, proteins were extracted for Western blot analysis. Approximately $5x10^6$ cells/mL of TSA and 5-Aza-treated Kasumi-1 cell suspensions were collected and centrifuged to obtain cell pellets. The cell pellets were washed with 3-5 mL of ice-cold phosphate-buffered saline (PBS) (Sigma Aldrich, MO, USA) by centrifuging at 10,000 × g for 5 minutes. 1-2 mL of ice-cold RIPA lysis buffer (Sigma Aldrich, MO, USA) was added to the cell pellets, which were then manually agitated in microfuge tubes for 30 minutes on ice with occasional vortexing. The samples were centrifuged again at 10,000 × g for 20 minutes. The supernatants were collected in a new collecting tube to obtain protein lysates. The protein concentration was determined using a reducing agent-compatible (RC) and detergent-compatible (DC) protein assay (Bio-Rad, CA, USA) according to the manufacturer's protocol.

2.7 WESTERN BLOT

500 µg of protein lysates per 200 µL were diluted with an equal volume of 2× Laemmli sample buffer (Bio-Rad, CA, USA) and heated at 95 °C for 5 minutes for loading onto the gel. 25 µg of protein lysate (per lane) was electrophoresed in 1× Running Buffer by denaturing Sodium dodecyl sulfate-polyacrylamide gel electrophoresis (SDS-PAGE) using Mini-PROTEAN Tetra cell electrophoresis set (Bio-Rad Laboratories, CA, USA) at 100 V, 200 mA, for 80 mins. Migrated proteins were blotted onto the PVDF membrane (Amersham, GE, Buckinghamshire, UK) using a semidry gel blot (Bio-Rad Laboratories, CA, USA) at 25 V, 250 mA for 1 hour. The membrane containing arrays of proteins was blocked by Blocking agent (5% Skimmed milk) (Anlene, Shah Alam, Malaysia) for 1 hour at room temperature (RT), washed with 0.1% Tween-PBS (0.1% (volume/volume) three times (10-15 mins each time interval), then were complexed with primary antibodies (anti-ANGPTL4, anti-TUBB2A, anti-histone H3, anti-histone H4 and anti-β-actin (**Table III**). The membranes were incubated overnight at 4°C on a reciprocating shaker. After incubation, the membranes were washed three times with 0.1% Tween-PBS and then incubated with secondary antibodies (HRP-linked IgG anti-Rabbit or IgG anti-Mouse) for 1 hour at room temperature (RT). The membranes were subsequently washed three times with 0.1% Tween-PBS. Immunoreactive bands on each membrane were detected using Amersham (enhanced chemiluminescence) ECL Western blotting detection agent (GE Healthcare, Buckinghamshire, UK) and images were captured by Fusion FX chemiluminescence imager (Vilber Lourmat, Marne-la Vallee, Collegien, France).

Table III: Human primary antibodies

Primary antibody	Specificity of primary antibody	Secondary antibody	Dilution	Molecular weight (~kDa)	Manufacturer
Anti-ANGPTL4	ANGPTL4 protein	Anti-rabbit	1:500	45.2	Sigma-Adrich™ Saint Louis, MO, USA
Anti-TUBB2A	β-tubulin TUBB2A protein	Anti-mouse	1:100	50	Calbiochem, San Diego, CA, USA
Anti-histone H3	Total histone H3 protein	Anti-rabbit	1:500	15	Sigma-Adrich™ Saint Louis, MO, USA
Anti-histone H4	Total histone H4 protein	Anti-rabbit	1:1000	11	Sigma-Adrich™ Saint Louis, MO, USA
Anti-β-actin	β-actin protein	Anti-rabbit	1:1000	45	Cell signalling, Danvers, MA, USA

2.8 STATISTICAL ANALYSES

Non-parametric tests, specifically the Mann-Whitney test, were used to compare differences between two independent groups, and the Kruskal-Wallis test was employed for multiple group comparisons. All statistical analyses were performed using the SPSS software package (Version 24, SPSS, Armonk, NY, USA), and a *p*-value <0.05 was considered significant.

3 RESULTS

3.1 DEMOGRAPHIC AND CLINICAL DATA OF AML PATIENTS

17 (32.7%) males, and 35 (67.3%) females were recruited, with a median age of 40 years at the time of diagnosis. The WBC median count was 28 × 10^9/L with values ranging from 1.3 to 346 × 10^9/L, with blast count (median 28%, range 1 to 97 %), Hb level (median 7.6 d/dL, range 3.2 to 211 d/dL), and platelet level (median 36.5 10^9/L, range 5 to 672 10^9/L). Cytogenetic profile of the patients showed 11 (21.2%) carry t(8;21), 12 (23.1) with carried t(15;17), 18 (34.6%) have normal cytogenetics (CN) and 11 (21.2%) patients presented with other cytogenetic aberration or/and complex cytogenetic. The patient classification according to the French-American-British (FAB) criteria were: M0 (n=1), M1 (n=3), M2 (n=11), M3 (n=11), M4 (n=9), M5 (n=8), M6 (n=1), M7 (n=0) and eight undefined (**Table IV**).

Table IV: Demographic and clinical data of aml patients

Demographic /clinical characteristics	All patients (Total= 52)
Gender (No., %)	
Male	17 (32.7%)
Female	35 (67.3%)
Age (median/ range)	40 (3 to 71 years)
WBC count (median/ range) (10^9/L)	28 (1.3 to 346)
Blast count (median/ range) (%)*	48 (1 to 97)
Hb level (median/ range) (g/dl)	7.6 (3.2 to 211)
Plt level (median/ range) (10^9/L)	36.5 (5 to 672)
FAB subtypes	
M0	1
M1	3
M2	11
M3	11
M4	9
M5	8
M6	1
M7	0
Undefined	8
Cytogenetic aberrations	
t(8;21) (No,%)	11 (21.2%)
t(15;17) (No,%)	12 (23.1%)
Normal cytogenetic (No, %)	18 (34.6%)
Others (No, %)	11 (21.2%)
Mutations	
FLT3-ITD	9 (17.3%)
NPM1	8 (15.4%)

WBC- white blood cell; Hb- hemoglobin; Plt-platelet; t-translocation; FAB- French American British; *Blast was derived from the peripheral blood

3.2 TRANSCRIPT LEVEL OF ANGPTL4 AND TUBB2A IN AML PATIENTS

The gene expression analysis of *ANGPTL4* and *TUBB2A* in AML patients revealed significant findings regarding their expression levels across different cytogenetic abnormalities (Kruskal-Wallis, p<0.05). The data were represented using box-whisker plots, which illustrated the median, highest, and lowest expression levels relative to normal healthy samples by relative quantitation (RQ) (Figure 1).

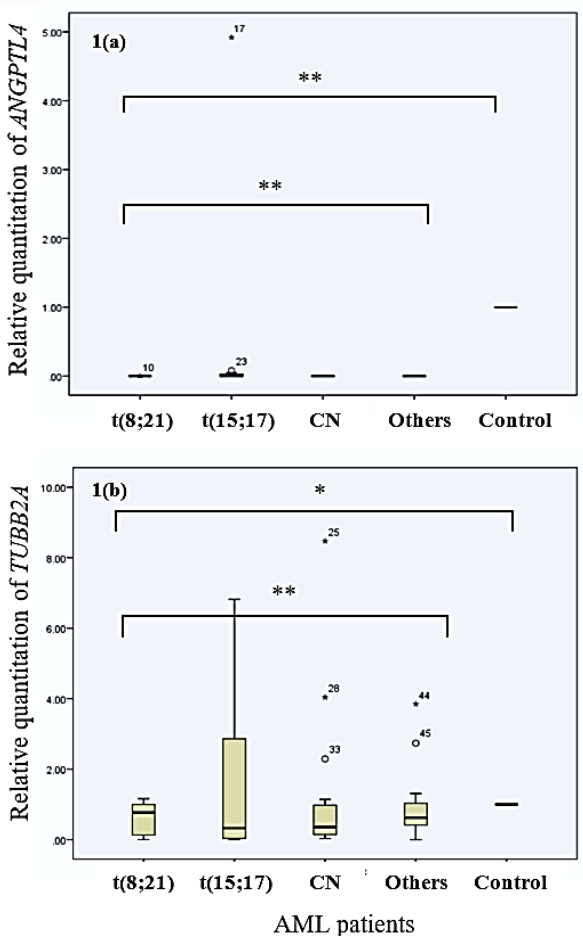

Figure 1: Quantitative real-time PCR (qRT-PCR). Box-and-whisker plots showing the relative quantification (RQ) of median expression levels for (a) *ANGPTL4* and (b) *TUBB2A* genes across all cytogenetic groups [t(8;21) (n=11), t(15;17) (n=12), CN (n=18), Others (n=11)] of AML in comparison to healthy individuals (Control). Expression outliers were shown by a small asterisk (*). Statistical significance was assessed using the Kruskal-Wallis test for multiple comparisons (*p<0.05, **p<0.01).

The analysis of RQ in AML patients was relative to healthy control samples (serving as a baseline level), which was set at 1. The results showed a significant difference in the median expression levels of *ANGPTL4* and *TUBB2A* among AML patients with different cytogenetic abnormalities (p<0.05). The median expression of *ANGPTL4* was extremely low, with a value of <0.001, whereas *TUBB2A* expression ranged between 0.33 and 0.77. Among the 52 AML patients analysed, 51 (98.1%) exhibited down-regulation of *ANGPTL4*. Downregulation of *ANGPTL4* was observed in all patients with t(8;21), t(15;17), and complex cytogenetics, as well as in the majority (94.4%) of patients with CN-AML. For *TUBB2A*, 38 patients (73.1%) showed down-regulation, while 14 patients (26.9%) exhibited up-regulated expression levels. Notably, among patients with down-regulated *TUBB2A*, a significant proportion (14 out of 18, or 77.8%) were cytogenetically normal. Detailed information on the number of patients with up-regulated and down-regulated expressions of *ANGPTL4* and *TUBB2A* across different cytogenetic groups is summarized in **Table V**.

Table V: Median expressions and regulations (up and down) of *ANGPTL4* and *TUBB2A* in AML

Expressions										Regulations			
Prognosis groups	Cytogenetic Abnormalities	n (%)	*ANGPTL4*				*TUBB2A*				*ANGPTL4*		*TUBB2A*	
			Median (SD)	$\chi2$ – statistic (df)	*p-value*[a]	*p-value*[b]	Median (SD)	$\chi2$ – statistic (df)	*p-value*[a]	*p-value*[b]	↑	↓	↑	↓
Favorable	t(8;21) (q22;q22)/ *AML1-ETO* or *RUNX1-CBFA2T1* (AML M4)	11 (21.2)	0.00 (0.001)			**0.00*** **	0.77 (0.47)			**0.009*** **	0 (0.0)	11 (100.0)	3 (27.3)	8 (72.7)
	t(15;17) (q22;q21)/ *PML-RARA* (APL, AML)	12 (23.1)	0.00 (0.261)	69.28 (4)	0.00***	**0.00*** **	0.33 (2.2)	9.99 (4)	0.04*	**0.05***	0 (0.0)	12 (100.0)	4 (33.3)	8 (66.7)
Intermediate	CN	18 (34.6)	0.00 (0.03)			**0.00*** **	0.36 (2.2)			**0.02***	1 (5.5)	**17 (94.4)**	4 (22.2)	**14 (77.8)**
Unfavorable	Others[¥]	11 (21.2)	0.00 (0.17)			**0.00*** **	0.62 (1.20)			**0.008*** **	0 (0.0)	11 (100.0)	3 (27.3)	8 (72.7)
Total		52 (100.0)									1 (1.9)	**51 (98.1)**	**14 (26.9)**	**38 (73.1)**

APL= acute promyelocytic leukemia, CN= Cytogenetically normal, ↑= up-regulation; ↓= down-regulation
[¥]Carry complex cytogenetic (consisting of ≥3 acquired chromosomal aberrations)
a. Mann-Whitney Test (2-tailed) was applied for two-group comparison, **p*<0.05, ***p*<0.001
b. Kruskal-Wallis Test was applied for multiple group comparison, **p<0.05, ***p<0.001*

3.3 DNA METHYLATION STATUS OF *ANGPTL4* AND *TUBB2A* IN AML PATIENTS

Methylation patterns exhibited either fully methylated regions (characterized by unconverted cytosine residues or a single peak for cytosine), partially methylated regions (characterized by double peaks for both cytosine and thymine residues), and unmethylated regions presented with a single thymine peak.

A total of 15 CpG sites were analysed for *ANGPTL4*, while 12 CpG sites were examined for *TUBB2A* in AML patients. Figure 2a demonstrates the BSP of the *ANGPTL4* gene, showing 7 out of 15 CpG sites. Patient P1 showed full methylation (100.0%) from CpG 1 to CpG 15, and patient P12 demonstrated partial methylation specifically at CpG 6 of the *ANGPTL4* promoter region, which represents 93.3% fully methylated CpGs. The methylated control and non-treated Kasumi-1 cells exhibited complete methylation (100.0%) at all analysed CpG dinucleotides. The healthy control sample showed a reduced number of methylated CpGs, with 9 out of 15 (60.0%) being fully methylated. In *TUBB2A*, 7 out of 12 analysed CpG sites (CpG 3-9) were shown to exhibit varying degrees of CpG methylation patterns, as observed in patients P1 and P6. Patient P1 showed 66.7% fully methylated CpGs, with partial methylation observed in CpG 3 and CpG 5.

In contrast, patient P6 showed a 50.0% fully methylated CpG area, with partial methylation observed in four CpGs: CpG 3, CpG 4, CpG 5, and CpG 6. While 2 CpGs: CpG 1 and 2 were found to be unmethylated in P1, and in P3 until P12. In contrast, the methylated control and untreated Kasumi-1 had full methylation (100.0%) at all CpG sites (Figure 2b). In the healthy control, the *TUBB2A* promoter exhibited a lower level of CpG methylation, with only 3 out of 12 CpGs (25.0%) being fully methylated. However, P8 showed a similar methylation pattern to the healthy control.

A summary of the overall methylation profiles for *ANGPTL4* and *TUBB2A* is shown in Figure 3, while detailed patient sequencing data for all CpGs are available in the *Appendix*. The fully methylated status of *ANGPTL4* and *TUBB2A,* along with their corresponding expression levels in representative AML patients, is shown in Table VI.

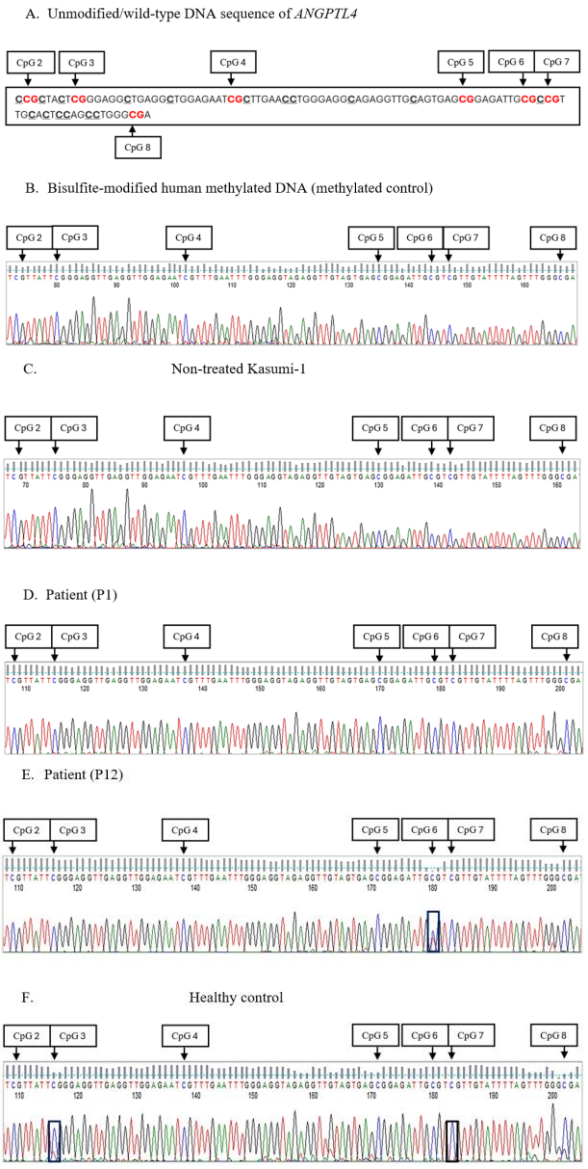

Figure 2 (a): A representative BSP analysis of 7 out of 15 CpG sites (arrows) within the *ANGPTL4* gene promoter region is shown. (A) The unmodified/wild-type DNA sequence of the *ANGPTL4* promoter is highlighted, with CpG sites in red (bold), and all unmethylated cytosines (C) are underlined, which were converted to thymines (T) after bisulfite modification. (B) In the modified DNA of the human methylated control, all methylated cytosines (blue) remained unchanged. (C) The modified DNA of untreated Kasumi-1 cells exhibited complete cytosine methylation. (D) The modified DNA of patient P1 showed fully methylated cytosines at the respective CpG sites. (E) The modified DNA of patient P12 exhibited partial methylation, as indicated by a double peak of cytosine and thymine at CpG 6 (boxed region). (F) The modified DNA of a healthy control showed a lower frequency of fully methylated cytosines (boxed region), in contrast to patient samples.

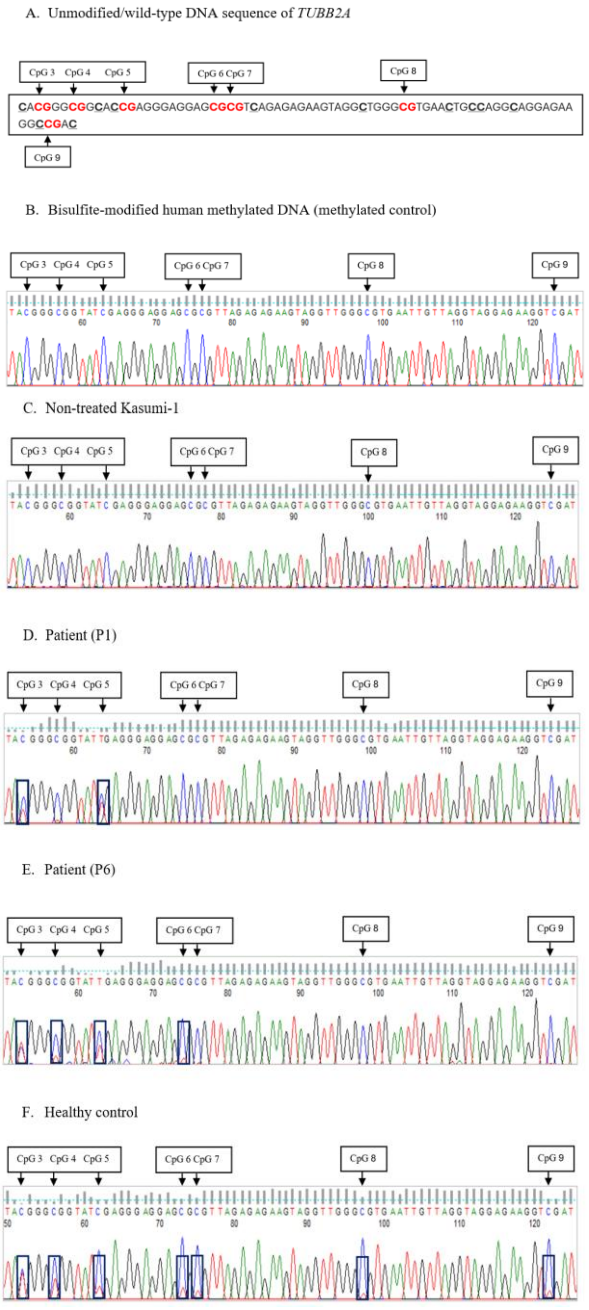

Figure 2 (b): A representative of the BSP results, analysing 7 out of 12 CpG sites (arrows) at the promoter region of the *TUBB2A* gene. (A) Unmodified/wild-type DNA sequence of *TUBB2A* promoter showing the CpG sites in red (bold) and all unmethylated cytosines (underlined) were converted to thymines after bisulfite modification (B). The modified DNA of the human methylated control showed that all methylated cytosines (blue) remained unconverted. (C) The modified DNA of the untreated Kasumi-1 cell harbored all cytosine methylation. (D, E) Modified DNA of selected AML patients, P1 and P6, with varying CpG site methylation degrees representing full and partial methylated cytosine (boxed region) (F). Modified DNA of a selected healthy control showed a higher degree of CpG's partial methylation compared to patient samples.

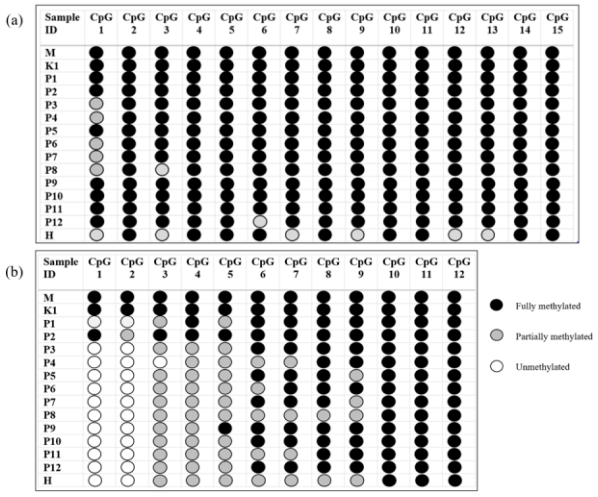

M= Universal human methylated DNA control, K1=Non-treated Kasumi-1 cell line, P=Patients, H= Healthy control

Figure 3: DNA methylation profile of *ANGPTL4* and *TUBB2A* gene's promoter region, analysed in the representative of 12 AML patients (P1-P12) in comparison to universal human methylated (M) DNA (positive control), non-treated Kasumi-1 cell (K1) and healthy control (negative control) (a) Schematic diagram of the DNA methylation pattern of 15 CpG sites of *ANGPTL4* showing a hypermethylated region. Nine out of 15 CpGs (60.0%) showed full methylation in a healthy control. (b) Schematic diagram of the DNA methylation pattern of 12 CpG sites of *TUBB2A* in AML patients, which showed different methylation patterns. The black circles, grey circles, and white circles represent the fully methylated, partially methylated, and unmethylated CpGs, respectively.

Table VI: *ANGPTL4* and *TUBB2A* methylation status in relation to their expression level

Patient's ID	Cytogenetics groups	*ANGPTL4*		*TUBB2A*	
		CpG fully methylation status (%)*	*Transcript level (↑/↓)*	*CpG fully methylation status* (%)*	*Transcript level (↑/↓)*
P1	CN	**15/15 (100.0)**	↓	**8/12 (66.7)**	↓
P2	Inv16	15/15 (100.0)	↓	11/12 (91.7)	↓
P3	CN	14/15 (93.3)	↓	7/12 (58.3)	↓
P4	t (8;21)	14/15 (93.3)	↓	5/12 (41.7)	↓
P5	t(15;17)	15/15 (100.0)	↓	6/12 (50.0)	↓
P6	C.N	14/15 (93.3)	↓	**6/12 (50.0)**	↓
P7	t(8;21)	14/15 (93.3)	↓	6/12 (50.0)	↓
P8	t(8;21)	13/15 (86.7)	↓	**3/12 (25.0)**	↓
P9	t(15;17)	15/15 (100.0)	↓	8/12 (66.7)	↓
P10	t(15;17)	15/15 (100.0)	↓	7/12 (58.3)	↑
P11	Complex	15/15 (100.0)	↓	5/12 (41.7)	↑
P12	Complex	**14/15 (93.3)**	↓	7/12 (58.3)	↓
Average fully methylated (%)		**14.4 (96.1)**	**↑=0, ↓=12 (100.0%)**	**6.6 (54.9)**	**↑=2, ↓=10 (83.3%)**
Healthy control		9/15 (60.0)		3/12 (25.0)	

NA= Not applicable, ↑ = Upregulated; ↓ = Downregulated
*Fully methylated out of the total CpG analysed

3.4 EXPRESSION OF FULL-LENGTH HUMAN ANGPTL4 AND TUBB2A PROTEINS

Due to the hypermethylated status and reduced expression of both *ANGPTL4* and *TUBB2A*, western blotting was performed to determine whether treatment with TSA (a HDAC inhibitor) or 5-Aza (a DNA methylation inhibitor) can restore their expression at the protein level. The results revealed an up-regulation of human ANGPTL4 and TUBB2A proteins, which corresponded to their mRNA levels after 24 hours of induction treatment with TSA and 5-Aza in the Kasumi-1 cell line. Untreated Kasumi-1 cells were used as the negative control (Figure 4).

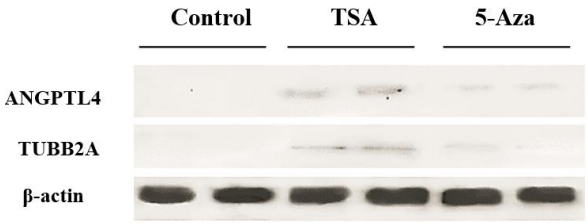

Figure 4: Western blot analysis of ANGPTL4 and TUBB2A expressions in Kasumi-1. The results showed that the expression levels of full-length human ANGPTL4 (45.2 kDa) and TUBB2A (50 kDa) proteins were increased after induction therapy with TSA and 5-Aza (in duplicate), compared with the non-treated Kasumi-1 cells, which served as a control. ß-Actin was used as a loading control, and the detection was performed using enhanced chemiluminescence.

3.5 TOTAL HISTONES H3 AND H4 CONTENT INCREASES UPON TSA TREATMENT

TSA treatment led to an increase in global histone H3 and H4 protein abundance, suggesting that HDAC inhibition may influence histone gene expression or chromatin dynamics through histone modifications [20]. The mechanism of action of TSA involves global histone H3 and H4 acetylation, as well as the reduction of DNA and H3K9 methylation, as previously reported in studies conducted in maize and human malignant cell lines [21, 22]. In this study, core histones H3 and H4 were upregulated in Kasumi-1 cells following TSA treatment, indicating an increase in global histone gene expression in response to HDAC inhibition. In contrast, treatment with 5-Aza, a DNA methylation inhibitor, did not directly affect histone levels, so such measurement was not relevant to its mechanism of action (**Figure 5**).

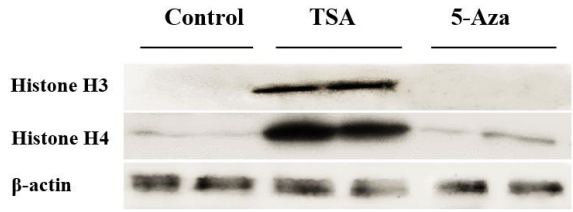

Figure 5: Western blot analysis of histone H3 and histone H4 protein expression in Kasumi-1 after induction therapy with TSA and 5-Aza (as a comparison control). Anti-histone H3 (15 kDa) and anti-histone H4 (11 kDa) antibodies were used to detect these proteins in the cell lysate of TSA-treated cells, in comparison to non-treated cells. Increased expression of the total histone H3 and H4 proteins was observed, marked by their upregulation upon TSA treatment, while their expression remained unchanged in 5-Aza treatment.Non-treated Kasumi-1 cells were used as a control, and ß-actin served as a loading control, detected using enhanced chemiluminescence

4 DISCUSSIONS

In our previous findings, we identified *ANGPTL4* and *TUBB2A* as putative TSGs that are commonly re-expressed in response to induction therapy with the epigenetic-modulating agents TSA and 5-Aza in Kasumi-1, a human acute myeloid leukemia (AML) cell line [13]. In the current study, we investigated the gene expression of *ANGPTL4* and *TUBB2A* in AML patients with various cytogenetic abnormalities, including t(8;21), t(15;17), CN, and complex cytogenetics. We also examined the involvement of epigenetic mechanisms by analyzing the DNA methylation epitype of these genes in AML.

The observed downregulation of *ANGPTL4* in nearly all AML patients (98.1%) suggests its potential role as a TSG. This consistent downregulation, regardless of cytogenetic abnormalities, highlights that the suppression of *ANGPTL4* is a common feature of all AML subtypes. It highlights *ANGPTL4* as a potential biomarker, particularly in identifying AML patients with aggressive or resistant forms [23]. *TUBB2A* shows more expression variability, with both down-regulated (73.1%) and up-regulated (26.9%) forms observed. This reflects its context-dependent role in AML, influenced by the specific cytogenetic subgroup [24] the higher proportion of *TUBB2A* down-regulation in CN patients (77.8%) suggests a potential association with genetic factors. In CN-AML, despite the lack of visible chromosomal changes, its heterogeneous nature leads to the accumulation of genetic and epigenetic lesions [25].

Different AML subclassifications are

associated with unique gene expression profiles that influence the epigenetic landscape, including DNA methylation patterns [26]. Genome-wide epigenetic profiling has uncovered AML subclassifications driven by DNA methylation, identifying 1755 differentially methylated regions (DMRs) correlated with known genetic abnormalities. These hyper- or hypomethylated genomic regions have significant prognostic value and may serve as potential biomarkers [27]. Methylation analysis revealed that the promoter region of *ANGPTL4* exhibited a high level of methylation, with 96.1% of CpG sites being fully methylated. In contrast, *TUBB2A* showed a moderate level of methylation, with 54.9% of CpG sites fully methylated (**Table VI**). These findings suggest differential methylation patterns that may influence the regulation of these genes in AML pathogenesis. The methylation status of CpG sites may have significant implications for disease pathogenesis. Fully methylated CpG sites typically silence gene expression by preventing transcription factor binding and promoting chromatin condensation. Partial methylation can lead to variable gene expression. This heterogeneity in methylation can result in a mixed population of cells with different levels of gene expression, potentially contributing to the complexity and aggressiveness of AML. At the same time, unmethylated CpG sites are typically associated with active gene expression [28].

The low expression of *ANGPTL4* in all AML patients in this study may be related to hypermethylation of its promoter region. All 12 patients analysed with DNA methylation had reduced expression of *ANGPTL4*. Hypermethylation acts as a repressive mechanism, inhibiting transcription and leading to the loss of gene function in cancer [29], as first described by Herman *et al.* (2003) [30]. Previous studies have demonstrated a similar relationship, where promoter hypermethylation of TSG, such as AT-rich interactive domain-containing protein 1A (*ARID1A*), was linked to low mRNA expression in invasive breast cancer [31], and hypermethylation of zinc finger protein 334 (*ZNF334*) was observed in hepatocellular carcinoma, correlating with its gene repression [32]. In contrast to *TUBB2A*, the fully CpG methylated sites have an average of 54.9%, and the remaining percentage contains partial methylation and unmethylated CpGs. Out of 12 patients, 2 have *TUBB2A* up-regulation, and one patient has an equal percentage of fully methylated CpG sites as a healthy control. These results suggest the heterogeneity of epigenetic changes in AML [33] and that *TUBB2A* is not significantly altered for that patient, within that gene location. This highlights the need for comprehensive analysis, such as the inclusion of patients at remission status or those experiencing relapse, for gene expression comparison, as a previous study revealed that in relapsed AML cases, there was a high epigenetic shift resulting in a change in overall methylation degree [34].

A 2023 study reported that DNA methylation profiles could define subtypes of AML, each associated with distinct prognostic and clinical features [35]. The interrelation of genetic and epigenetic events has been described in gliomas, where the 2-hydroxyglutarate oncometabolite resulting from an isocitrate dehydrogenase (*IDH*) mutation obstructs the DNA demethylating mechanism, leading to uncontrolled DNA methylation. This consequently leads to the loss of CCCTC-binding factor 11, also known as zinc finger protein (*CTCF*), and the upregulation of the oncogene platelet-derived growth factor receptor A (*PDGFRA*) in gliomas [36].

In t(8;21)-positive AML, the AML1-ETO fusion protein acts as a transcriptional repressor by recruiting co-repressor complexes, including nuclear receptor co-repressor (N-CoR), silencing mediator of retinoic acid and thyroid hormone receptor (SMRT), and HDACs, through its MYND domain. This recruitment leads to chromatin remodeling and gene silencing [37]. Our study demonstrates that treatment with TSA, an HDAC inhibitor, upregulates global histone gene expression in response to HDAC inhibition, leading to the reactivation of *ANGPTL4* and *TUBB2A* expression at both the mRNA and protein levels. The PML-RARA fusion protein, arising from the t(15;17) translocation, recruits various transcriptional repressors, including HDACs and DNMTs, which contribute to the silencing of differentiation-related genes [38]. The evidence from previous studies supports the relationship between genetic and epigenetic control of gene transcription.

In other malignancies, methylation-associated gene silencing of *ANGPTL4* has been observed in gastric cancer, where its overexpression suppresses tumorigenicity and angiogenesis in vivo [39]. This has also been

observed in hepatocellular carcinoma (HCC) patients [40] and colorectal cancer patients [41] with down-regulation significantly associated with advanced tumor stage, metastasis, and poor differentiation. The study also recorded higher *ANGPTL4* methylation frequency in HCC patients compared to healthy control. *ANGPTL4* was also hypermethylated in primary breast carcinoma cells. Treatment with epigenetic drugs significantly reduced the number of *ANGPTL4* methylated regions [42]. No studies have yet explored the epigenetic profile of *ANGPTL4* in hematological malignancies, making this the first study to report the expression and methylation profile of *ANGPTL4* in AML.

Regarding *TUBB2A*, the gene has gained attention for its role in brain tumors and cortical malformations, with specific mutations identified in both alpha and beta-tubulin genes that correlate with these conditions. These mutations can disrupt microtubule dynamics, which are essential for various cellular processes such as mitosis and intracellular transport [40, 43]. Recent studies have identified eight novel mutations and one recurrent mutation in the *TUBB2A* gene among patients with brain malformations [44]. In breast cancer cells, resistance to taxane chemotherapy has been linked to abnormal protein folding of tubulins, which is influenced by mutations and dysfunctions in tubulin-specific chaperones, including *TUBB2A* [45]. Antimicrotubule agents such as vincristine, paclitaxel, and docetaxel are widely used in breast cancer treatment, targeting the beta-tubulin subunit of microtubules. In the MCF-7 breast cancer cell line, mutations in the beta-tubulin isotype gene, *TUBB*, have been associated with resistance to these drugs [46]. Despite these findings, there is a notable gap in the literature regarding the role of *TUBB2A* in hematological malignancies, particularly AML. To date, no studies have specifically addressed the gene mutation state or expression profiles within this context. Given *TUBB2A*'s involvement in microtubule formation and its association with drug resistance in solid tumors, investigating its potential impact on AML pathogenesis and treatment resistance could provide valuable insights.

The observed upregulation of ANGPTL4 and TUBB2A proteins following TSA and 5-Aza treatment in Kasumi-1 cells supports the involvement of epigenetic mechanisms in the repression of these genes in AML. This aligns with the hypermethylated status and previously reported downregulation of *ANGPTL4* mRNA in various cancer types [39-41], and also suggests a potential role for *TUBB2A* in cancer pathogenesis that warrants further investigation. TSA, an HDAC inhibitor, likely facilitated gene re-expression through increased histone acetylation and chromatin relaxation [21, 22, 47], while 5-Aza, a DNA methyltransferase inhibitor, may have reversed promoter hypermethylation. The concordance between mRNA and protein expression suggests that epigenetic mechanisms may influence both transcriptional and post-transcriptional regulation. Collectively, these findings underscore the therapeutic potential of targeting epigenetic regulators to reactivate silenced genes in leukemic cells.

This study also observed an up-regulation of core histones H3 and H4 proteins in Kasumi-1 cells following TSA treatment, indicating that TSA effectively inhibits histone deacetylation by targeting the HDAC molecule. While histone modifications such as acetylation (e.g., H4ac) and methylation (e.g., H3K9me) are typically assessed using modification-specific antibodies that show elevation [21, 22, 48], the current study employed antibodies recognizing total/core histone H3 and H4. Core histone proteins are generally considered stable and often serve as loading controls in chromatin studies. The observed upregulation may reflect an indirect effect of TSA on histone gene expression, potentially mediated through alterations in cell cycle regulation or chromatin remodelling [51], and changes in histone density that affect global histone acetylation [49]. Previous studies have reported that HDAC inhibition can influence histone mRNA and protein levels during S-phase progression and nucleosome turnover. For instance, a study demonstrated that TSA treatment led to increased histone acetylation at replication origins, which was associated with changes in replication initiation activity, suggesting a link between histone acetylation and DNA replication dynamics [21, 50]. These findings warrant further investigation using histone modification-specific antibodies to clarify whether epigenetic changes are directly responsible for the reactivation of the *ANGPTL4* and *TUBB2A* genes.

By inhibiting HDACs, TSA prevents the removal of acetyl groups from histones, resulting

in the hyperacetylation of histones and subsequent active gene expression. This finding suggests that the Kasumi-1 cell line or AML initially exhibits low baseline levels of histones H3 and H4. As stated previously, the mechanism of gene activation involves an increase in global histone H4 acetylation and a decrease in DNA and H3K9 methylation [21, 47]. Reduced acetylation of histone proteins due to dysregulation of HDAC was observed in AML cases, as reported in previous studies [51, 52]. In many cancers, histone acetylation is commonly reduced, leading to a tight, repressed chromatin structure and repression of TSGs expression [52]. Furthermore, the presence of repressive histone modifications is often accompanied by DNA hypermethylation, further supporting the downregulation of TSGs [31, 53].

This study has several limitations. First, the small sample size within each cytogenetic group limits the accuracy and coverage of determining the prevalence of *ANGPTL4* and *TUBB2A* expression. This limited recruitment is due to single-center study and the low prevalence of AML cases in our region. Second, DNA methylation analysis was conducted in only 12 patients due to insufficient DNA samples. Third, the methylation analysis was based solely on bisulfite sequencing. Incorporating additional methylation platforms could enhance the reliability of the findings. For a more precise evaluation of histone dynamics following TSA treatment, future studies should assess specific post-translational modifications such as histone H4 acetylation (H4ac) and histone H3 lysine 9 methylation (H3K9me). This would provide clearer insight into the epigenetic changes contributing to gene regulation. Future studies should include larger patient cohorts recruited from multiple centers and employ a range of DNA methylation assays and histone modification analyses to enhance the robustness and generalizability of the findings.

5 CONCLUSION

This study investigates the expression and methylation profiles of *ANGPTL4* and *TUBB2A* in AML patients, revealing that most patients exhibit reduced expression of both genes, likely due to hypermethylation in their promoter regions. This downregulation may contribute to the persistence of leukemic stem cells, highlighting the potential epigenetic-modulating role of *ANGPTL4* and *TUBB2A* in AML pathogenesis. Furthermore, the observed upregulation of core histone H3 and H4 following TSA treatment suggests changes in histone dynamics that may be linked to dysregulated HDAC activity in AML.

In conclusion, this study enhances our understanding of epigenetic regulation in leukemia and highlights the potential of *ANGPTL4* and *TUBB2A* as novel biomarkers or therapeutic targets. With further validation, these findings could inform the development of improved diagnostic tools and epigenetic-based treatment strategies. Future research should focus on preclinical evaluation of demethylating agents targeting *ANGPTL4* and *TUBB2A* promoter hypermethylation, as well as on investigating their roles in leukemic stem cell maintenance and therapy resistance.

APPENDIX

See appendix I.

ACKNOWLEDGEMENT

This study was supported by Research University Grants (1001/PPSP/8012247) and (1001/PPSP/813050) from Universiti Sains Malaysia (USM), Malaysia. Mat Jusoh Siti Asmaa was supported by MyBrain15 scholarship from the Ministry of Education, Malaysia.

REFERENCES

[1] S. E. Gutierrez and F. A. Romero-Oliva. Epigenetic changes: a common theme in acute myelogenous leukemogenesis. Journal of Hematology & Oncology, 2013. 6(1), pp. 57.
[2] A. Nebbioso, et al. Cancer epigenetics: Moving forward. PLOS Genetics, 2018. 14(6), pp. e1007362.
[3] M. Fardi, S. Solali, and M. Farshdousti Hagh. Epigenetic mechanisms as a new approach in cancer treatment: An updated review. Genes & Diseases, 2018. 5(4), pp. 304-311.
[4] A. P. Feinberg and A. Levchenko. Epigenetics as a mediator of plasticity in cancer. Science, 2023. 379(6632), pp. eaaw3835.
[5] V. Davalos and M. Esteller. Cancer epigenetics in clinical practice. CA: A Cancer Journal for Clinicians, 2023. 73(4), pp. 376-424.
[6] J. G. Herman and S. B. Baylin. Promoter-region hypermethylation and gene silencing in human cancer. Current Topics in Microbiology and Immunology, 2000. 249, pp. 35-54.
[7] M. Rodríguez-Paredes and M. Esteller. Cancer epigenetics reaches mainstream oncology. Nature Medicine, 2011. 17(3), pp. 330-339.
[8] S. C. Wu and Y. Zhang. Active DNA demethylation: many roads lead to Rome. Nature Reviews: Molecular Cell Biology 2010. 11(9), pp. 607-620.
[9] A. Kazanets, et al. Epigenetic silencing of tumor suppressor genes: Paradigms, puzzles, and potential.

Biochimica et Biophysica Acta (BBA) - Reviews on Cancer, 2016. 1865(2), pp. 275-288.
[10] X. Xu, et al. Metabolic reprogramming and epigenetic modifications in cancer: from the impacts and mechanisms to the treatment potential. Experimental & Molecular Medicine, 2023. 55(7), pp. 1357-1370.
[11] Y. Chen, et al. The role of histone methylation in the development of digestive cancers: a potential direction for cancer management. Signal transduction and targeted therapy, 2020. 5(1), pp. 143.
[12] H. Matsushita, et al. In vivo analysis of the role of aberrant histone deacetylase recruitment and RARα blockade in the pathogenesis of acute promyelocytic leukemia. The Journal of experimental medicine, 2006. 203(4), pp. 821-828.
[13] M. J. S. Asmaa, et al. Transcriptomic Profiles of MV4-11 and Kasumi 1 Acute Myeloid Leukemia Cell Lines Modulated by Epigenetic Modifiers Trichostatin A and 5-Azacytidine. International Journal of Hematology-Oncology and Stem Cell Research, 2020. 14(1), pp. 72–92.
[14] National Cancer for Biotechnology Information (NCBI) Gene ID: 51129. ANGPTL4 angiopoietin like 4 [Homo sapiens (human)],. 2018 14/10/2018 26 June 2018]; Available from: https://www.ncbi.nlm.nih.gov/51129.
[15] The University of Texas Health Science Center., Tumor suppressor gene database. 2016 School of Biomedical Informatics, Houston, US.
[16] M. Zhao, et al. TSGene 2.0: an updated literature-based knowledgebase for tumor suppressor genes. Nucleic Acids Research, 2016. 44(D1), pp. D1023-D1031.
[17] National Cancer for Biotechnology Information (NCBI) Gene ID: 7280. TUBB2A tubulin beta 2A class IIa [Homo sapiens (human)]. 2015 21-Jun-2018 24/6/2018]; Available from: https://www.ncbi.nlm.nih.gov/gene/7280.
[18] L. Chen, et al. Inferring Novel Tumor Suppressor Genes with a Protein-Protein Interaction Network and Network Diffusion Algorithms. Mol Ther Methods Clin Dev, 2018. 10, pp. 57-67.
[19] R. Parrish, J. J. Day, and F. D. Lubin. Direct bisulfite sequencing for examination of DNA methylation patterns with gene and nucleotide resolution from brain tissues. Current Protocols in Neuroscience, 2012. CHAPTER 7, pp. Unit7.24.
[20] F. Cozzolino, et al. Lysines Acetylome and Methylome Profiling of H3 and H4 Histones in Trichostatin A—Treated Stem Cells. International Journal of Molecular Sciences, 2021. 22, DOI: 10.3390/ijms22042063.
[21] M. G. Kemp, et al. The histone deacetylase inhibitor trichostatin A alters the pattern of DNA replication origin activity in human cells. Nucleic Acids Res, 2005. 33(1), pp. 325-36.
[22] Y. Zhou, et al. Trichostatin A Promotes Cytotoxicity of Cisplatin, as Evidenced by Enhanced Apoptosis/Cell Death Markers. Molecules, 2024. 29, DOI: 10.3390/molecules29112623.
[23] M. Levin, et al. Deciphering molecular mechanisms underlying chemoresistance in relapsed AML patients: towards precision medicine overcoming drug resistance. Cancer Cell International, 2021. 21(1), pp. 53.
[24] J. Bruneau and T. J. Molina. WHO classification of tumors of hematopoietic and lymphoid tissues. Hematopathology, 2020, pp. 501-505.
[25] K. Mrózek, et al. Clinical relevance of mutations and gene-expression changes in adult acute myeloid leukemia with normal cytogenetics: are we ready for a prognostically prioritized molecular classification? Blood, 2006. 109(2), pp. 431-448.
[26] S. Vosberg, et al. DNA Methylation Profiling of AML Reveals Epigenetic Subgroups with Distinct Clinical Outcome. Blood, 2019. 134(Supplement_1), pp. 2715-2715.
[27] M. Schmutz, et al. Predictive value of DNA methylation patterns in AML patients treated with an azacytidine containing induction regimen. Clinical Epigenetics, 2023. 15(1), pp. 171.
[28] O. Taryma-Leśniak, et al. Methylation patterns at the adjacent CpG sites within enhancers are a part of cell identity. Epigenetics & Chromatin, 2024. 17(1), pp. 30.
[29] S. B. Baylin and J. E. Ohm. Epigenetic gene silencing in cancer – a mechanism for early oncogenic pathway addiction? Nature Reviews Cancer, 2006. 6(2), pp. 107-116.
[30] J. G. Herman and S. B. Baylin. Gene silencing in cancer in association with promoter hypermethylation. New England Journal of Medicine, 2003. 349(21), pp. 2042-2054.
[31] X. Zhang, et al. Promoter Hypermethylation of ARID1A Gene Is Responsible for Its Low mRNA Expression in Many Invasive Breast Cancers. PLOS ONE, 2013. 8(1), pp. e53931.
[32] D. Sun, et al. DNA hypermethylation modification promotes the development of hepatocellular carcinoma by depressing the tumor suppressor gene ZNF334. Cell Death & Disease, 2022. 13(5), pp. 446.
[33] Y. Li, et al. Clinical implications of genome-wide DNA methylation studies in acute myeloid leukemia. Journal of Hematology & Oncology, 2017. 10(1), pp. 41.
[34] S. Li, C. E. Mason, and A. Melnick. Genetic and epigenetic heterogeneity in acute myeloid leukemia. Current opinion in genetics & development, 2016. 36, pp. 100-106.
[35] J. Jian, et al. DNA methylation-based subtypes of acute myeloid leukemia with distinct prognosis and clinical features. Clinical and Experimental Medicine, 2023. 23(6), pp. 2639-2649.
[36] H. Yan, et al. IDH1 and IDH2 mutations in gliomas. New England journal of medicine, 2009. 360(8), pp. 765-773.
[37] Y. Liu, et al. Structural basis for recognition of SMRT/N-CoR by the MYND domain and its contribution to AML1/ETO's activity. Cancer Cell, 2007. 11(6), pp. 483-97.
[38] U. Testa and E. Pelosi, Function of PML-RARA in Acute Promyelocytic Leukemia, in Transcription factors in blood cell development, T. Borggrefe and B.D. Giaimo, Editors. 2024, Springer Nature Switzerland: Cham. p. 321-339.
[39] E. Okochi-Takada, et al. ANGPTL4 is a secreted tumor suppressor that inhibits angiogenesis. Oncogene, 2014. 33(17), pp. 2273-8.
[40] Thomas D. Cushion, et al. De Novo Mutations in the Beta-Tubulin Gene TUBB2A Cause Simplified Gyral Patterning and Infantile-Onset Epilepsy. American Journal of Human Genetics, 2014. 94(4), pp. 634-641.
[41] K. Zhang, et al. DNA methylation mediated down-regulation of ANGPTL4 promotes colorectal cancer metastasis by activating the ERK pathway. J Cancer, 2021. 12(18), pp. 5473-5485.
[42] N. Hattori, et al. Methylation silencing of angiopoietin-like 4 in rat and human mammary carcinomas. Cancer Science, 2011. 102(7), pp. 1337-43.
[43] R. Romaniello, et al. Mutations in α- and β-tubulin encoding genes: Implications in brain malformations. Brain and Development, 2015. 37(3), pp. 273-280.
[44] S. Brock, et al. Defining the phenotypical spectrum associated with variants in TUBB2A. Journal of Medical Genetics, 2021. 58(1), pp. 33.

[45] B. Nami and Z. Wang. Genetics and Expression Profile of the Tubulin Gene Superfamily in Breast Cancer Subtypes and Its Relation to Taxane Resistance. Cancers (Basel), 2018. 10(8).
[46] O. D. Iseri and U. Gunduz. Drug resistant MCF-7 cells have altered expression levels of ß-tubulin isotypes and mutations in TUBB gene. International Journal of Hematology and Oncology, 2010. 34(1), pp. 075-083.
[47] F. Yang, et al. Trichostatin A and 5-azacytidine both cause an increase in global histone H4 acetylation and a decrease in global DNA and H3K9 methylation during mitosis in maize. BMC Plant Biology, 2010. 10(1), pp. 178.
[48] L. Pufahl, et al. Trichostatin A induces 5-lipoxygenase promoter activity and mRNA expression via inhibition of histone deacetylase 2 and 3. Journal of Cellular and Molecular Medicine, 2012. 16(7), pp. 1461-1473.
[49] C. Bruhn, G. Bastianello, and M. Foiani. Cancer cell histone density links global histone acetylation, mitochondrial proteome and histone acetylase inhibitor sensitivity. Communications Biology, 2022. 5(1), pp. 882.
[50] M. Koprinarova, M. Schnekenburger, and M. Diederich. Role of Histone Acetylation in Cell Cycle Regulation. Current Topics in Medicinal Chemistry, 2016. 16(7), pp. 732-744.
[51] C. Zhang, et al. Histone acetylation: novel target for the treatment of acute lymphoblastic leukemia. Clin Epigenetics, 2015. 7, pp. 117.
[52] P. Wang, Z. Wang, and J. Liu. Role of HDACs in normal and malignant hematopoiesis. Molecular cancer, 2020. 19, pp. 1-21.
[53] L. Chen, S. Liu, and Y. Tao. Regulating tumor suppressor genes: post-translational modifications. Signal Transduction and Targeted Therapy, 2020. 5(1), pp. 90.